A high-precision approach to reconstruct distribution of relaxation times from electrochemical impedance spectroscopy

Yanxiang Zhang,[a]* Yu Chen,[b] Mei Li,[c] Mufu Yan,[a] Meng Ni,[d] Changrong Xia[c]*

[a] National Key Laboratory for Precision Hot Processing of Metals, School of Materials Science and Engineering, Harbin Institute of Technology, Harbin 150001, China

[b] Center for Innovative Fuel Cell and Battery Technologies, School of Materials Science and Engineering, Georgia Institute of Technology, GA 30332-0245, USA

[c] CAS Key Laboratory of Materials for Energy Conversion, Department of Materials Science and Engineering, University of Science and Technology of China, Hefei, 230026, China

[d] Building Energy Research Group, Department of Building and Real Estate, The Hong Kong Polytechnic University, Hung Hom, Kowloon, Hong Kong, China

* Authors to whom correspondence should be addressed:

Tel: +86 451 86418617, fax: +86 451 86413922, E-mail address: hitzhang@hit.edu.cn (Y. Zhang); Tel.: +86 551 3607475; Fax: +86 551 3601592, Email: xiacr@ustc.edu.cn (C.R. Xia).

Abstract

A new Tikhonov regularization approach without adjusting parameters is proposed for reconstructing distribution of relaxation time (DRT). It is capable of eliminating the pseudo peaks and capturing discontinuities in the DRT, making it feasible to resolve the number and the nature of electrochemical processes without making assumptions.

Keywords

Distribution of relaxation time (DRT); Impedance spectroscopy; Fuel cells

Introduction

Electrochemical impedance spectroscopy (EIS) is the most frequently used methodology to study the electrolyte/electrode behaviours in electrochemical devices, for instance fuel cells, electrolyzers, batteries, and capacitors [1]. The electrochemical processes embedded in the EIS are usually characterized using some well-known representations of the EIS, for example the Nyquist plot, the imaginary impedance *vs.* frequency plot, etc. The number and nature of the electrochemical processes are identified by examining the number of arcs in the EIS curve and by curve-fitting with an equivalent circuit model, respectively [2]. However, this approach could underestimate the number of processes and oversimplify their electrochemical nature, as EIS curve is an integration of the responses of all the elementary processes and some elementary processes may not be shown in the curve [3]. In recent years, distribution

of relaxation times (DRT) has shown remarkable capability to differentiate the electrochemical processes and thus is a powerful tool for analyzing electrochemical power sources. The DRT is defined implicitly by [4, 5],

$$-Z''(\omega) = \int_0^\infty \frac{\omega F(\tau)/\ln(10)}{1+(\omega\tau)^2} d\tau \quad (1)$$

where $F(\tau)$ is the DRT function at the relaxation time τ, and $Z''(\omega)$ denotes the imaginary part of the impedance at the angular frequency ω. Characterized by individual peaks in the plot of $F(\tau)$ versus $\log_{10}(\tau)$, the electrochemical processes can be differentiated from each other to the most extent. The integral area of a specific peak corresponds to the resistance of a specific elementary process. Although conceptually simple, the DRT function has to be reconstructed numerically from the EIS data by solving Eq. 1, which is very challenging. The Tikhonov regularization is commonly used for reconstructing the DRT function [4-11]. By optimizing the regularization factor, the DRT function can be reconstructed properly. However, pseudo peaks are sometimes created in the reconstructed DRT plot, limiting the accuracy of this method. Very recently, Ciucci et al. proposed a Bayesian approach by considering the regularization factor as a hyper prior function of roughness of the reconstructed DRT function [12]. It was found that the reconstructed DRT functions were identical to the ideally analytical DRT solutions with proper parameters in the hyper prior function. However, as adjusting parameters are used, the accuracy of the results could be uncertain if the parameters were not properly set.

In this work, we propose a new Tikhonov regularization approach without adjusting parameters. The optimal DRT solution without pseudo peaks and the

distribution of regularization factor can be obtained simultaneously by using a well-established algorithm. Using this approach, the Gerischer type DRT can be resolved clearly from the impedance of a symmetric $La_{0.6}Sr_{0.4}Co_{0.2}Fe_{0.8}O_3$ (LSCF)/$Ce_{0.9}Sm_{0.1}O_{1.95}$ (SDC)/LSCF solid oxide cell, and the cathodic and anodic processes for a Ni-$Zr_{0.92}Y_{0.08}O_{1.96}$ (YSZ)/YSZ/$(La_{0.80}Sr_{0.20})_{0.95}MnO_{3-x}$ (LSM)-YSZ solid oxide cell are well separated. Finally, we propose a generic Tikhonov approach with higher orders distributions of regularization factor. The present Tikhonov approach is the first-order approximation of the generic Tikhonov approach.

Theory

Theoretically, the DRT function $F(\tau)$ can be reconstructed by Eq. 1 only if the impedance is linear, causal, and stable [13]. In other words, the real part $Z'(\omega)$ and the imaginary part $Z''(\omega)$ should yield Kramers-Kronig relations, which can be validated using ZSimpWin software, or the computer programs developed by B.A. Boukamp or Ivers-Tiffée group. The reconstruction is to calculate the discrete DRT set $\{F(\tau_n) \mid n = 1, 2, ..., N\}$ using the discrete impedance set $\{Z''(\omega_n) \mid n = 1, 2, ..., N\}$, where $\tau_n = 1/\omega_n$ and N denotes the number of the discrete impedance points collected. In the literature, $\{F(\tau_n) \mid n = 1, 2, ..., N\}$ was calculated by using a constant regularization factor. However, the reconstruction quality depends upon the value of regularization factor. In this work, we postulate a distribution of regularization factor (DRF), $\{\lambda_0(\tau_n) \mid n = 2, 3, ..., N\text{-}1\}$ across the relaxation timescale. Combining with the discretization of Eq. 1, the optimal DRT and DRF could be obtained by minimizing the objective function *err*

using a new Tikhonov regularization, given by the following matrix formulation,

$$err = (\boldsymbol{\Gamma}\mathbf{F} - \mathbf{Z})^{\mathrm{T}} (\boldsymbol{\Gamma}\mathbf{F} - \mathbf{Z}) + (\mathbf{D}_0\mathbf{F})^{\mathrm{T}} diag(\boldsymbol{\lambda}_0)^2 (\mathbf{D}_0\mathbf{F}) + \mathbf{F}^{\mathrm{T}}\mathbf{F}(\mathbf{D}_1\boldsymbol{\lambda}_0)^{\mathrm{T}} (\mathbf{D}_1\boldsymbol{\lambda}_0) \quad (2)$$

where $\mathbf{F}$ is a non-negative column vector of N components, with $\mathbf{F}_n = F(\tau_n)$; $\boldsymbol{\lambda}_0$ is a column vector of (N-2) components, with $\boldsymbol{\lambda}_{0n} = \lambda_0(\tau_n)$ for n = 2, 3, ..., N-1; $\boldsymbol{\Gamma}$ is a (N+1)×N matrix, with $\boldsymbol{\Gamma}_{i,j} = (\omega_i/\omega_j)/[ppd(1+\omega_i^2/\omega_j^2)]$ for i = 1, 2, ..., N and j = 1, 2, ..., N, and $\boldsymbol{\Gamma}_{N+1,j} = 1/ppd$ for j = 1, 2, ..., N; ppd denotes the number of impedance points per frequency decade; $\mathbf{Z}$ is a column vector of (N+1) components, with $\mathbf{Z}_n = -Z''(\omega_n)$ for n = 1, 2, ..., N, and $\mathbf{Z}_{N+1}$ is the entire polarization resistance of the impedance (R_p). When the absolute values of $Z''(\omega_1)$ and $Z''(\omega_N)$ are close to zero, say smaller than 1% of $|Z'(\omega_1) - Z'(\omega_N)|$, $\mathbf{Z}_{N+1}$ can be represented by $|Z'(\omega_1) - Z'(\omega_N)|$. Otherwise, R_p may be estimated by extrapolation, such as the method proposed by J. Matthew Esteban and Mark E. Orazem [14]; $\mathbf{D}_0$ is a (N-2)×N matrix, with $\mathbf{D}_{0n,[n,n+1,n+2]}$ = [-1 2 -1] and the other components of $\mathbf{D}_0$ are zeros; $\mathbf{D}_1$ is a (N-4)×(N-2) matrix, with $\mathbf{D}_{1n,[n,n+1,n+2]}$ = [-1 2 -1] and the other components of $\mathbf{D}_1$ are zeros; the superscript $^{\mathrm{T}}$ is short for transposition of matrix. It is noted that the objective function degrades into the one of the conventional Tikhonov approach when the DRF is a constant (say λ) throughout the timescale. In this case, λ^2 corresponds to the regularization factor of the conventional Tikhonov approach. The objective function err contains three terms. The first term represents the deviation between the original impedance $\mathbf{Z}$ and the one back-calculated by the DRT function $\boldsymbol{\Gamma}\mathbf{F}$. The second term represents the roughness of the DRT function, weighted by the DRF function. This term is the core of the new regularization. The interplay between DRT and DRF across the relaxation timescale can be captured. For

example, minimizing *err* permits the roughness around the discontinuities of DRT (if any) being significant by decreasing the corresponding DRF values. Thus, the discontinuities of DRT could be captured, which will be verified in what follows. The discontinuities in the DRT function are common for electrochemical cells, especially those containing mixed ionic-electronic catalysts, for example LSCF [15]. In addition, this regularization is also capable of capturing the continuities in the DRT function by increasing the corresponding DRF values. Thus, pseudo peaks can be avoided, which will also be verified in what follows. The third term represents the roughness of the DRF function. That is, we expect the DRF is a continuous function of relaxation time. Essentially, a continuous DRF means the strength of the regularization at neighboring relaxation times does not vary apparently. This term is crucial to preventing over-fitting of the DRT function. Well-established algorithms are available to minimize Eq. 2. One recommendation is the 'fmincon' function with the trust-region-reflective algorithm built in Matlab package, as used in this work. The trust-region-reflective algorithm is simple yet powerful in optimization, especially in minimizing the objective functions like Eq. 2, which have constrains of only bonds ($\mathbf{F} \geq 0$) and analytic formulas for gradient and Hessian matrix [16]. The initial value of DRF should be sufficiently high, so that the regularization during the iteration is strong enough to prevent over-fitting of DRT. We use an uniform DRT ($\mathbf{F}_i = R_\mathrm{p} \times ppd/N$) and an uniform DRF ($\boldsymbol{\lambda}_{0i} = ppd/N$) as the initial values. One can also use the optimized solutions by the conventional Tikhonov regularization as the initial values. The two choices of initial values eventually converge to nearly identical solutions.

Results and discussion

We test this approach by using three case studies. The first case uses the synthetic impedances of typical elemental circuits and an integrated circuit model to validate the accuracy of the new approach and to show the robustness against noise. The second case uses the impedance of a symmetric LSCF/SDC/LSCF solid oxide cell to show the capability of capturing the discontinuity in DRT function and the capability of eliminating pseudo peaks for use in realistic impedance. The third case uses the impedances of a Ni-YSZ/YSZ/LSM-YSZ solid oxide cell to show the merits of resolving electrochemical processes.

Fig. 1 a, b and c show respectively the reconstructed DRT functions by the new approach and the conventional approach with the regularization factor λ^2 being the averaged DRF value of the new approach and the ideally analytic DRT solutions for a RQ element, a finite length Warburg (FLW) element, and a Gerischer (G) element, which are usually used in analyzing solid oxide fuel cells. It is shown that the reconstructed DRT solutions by the new approach do not contain pseudo peaks and the non-continuity at the characteristic time of the G element is captured. By the conventional approach, it is tough to differentiate the FLW element and the G element as shown in Fig. 1b and c, as well as shown in ref. [11]. While, the new approach is more precise and makes it feasible to differentiate these elements by their shapes of reconstructed DRT function. The new approach is applicable for generic impedance. Fig. 1d shows the reconstruction result for a circuit model consisting of five elemental

circuits, mimicking a solid oxide fuel cell [11]. It is shown that all the processes are resolved correctly by the new approach with higher accuracy as compared to the conventional approach. In addition, an advantage over the Bayesian approach by Ciucci et al. is that no adjusting parameter is needed to get the DRT function and the DRF function. The DRF functions for the four synthetic impedances are shown in Fig. 2. The DRF determined intelligently by the optimization permits a flexible regularization strength on the DRT across the relaxation timescale. Referring to the DRT functions, we can see that smaller DRF values ($\lambda^2 < 10^{-3}$) correspond to a finer DRT structure, and the local minima of DRF indicate the discontinuities and/or the peaks of DRT. However, the electrochemical significance of the DRF needs to be further explored.

In addition to the accuracy, the robustness against noise is also important for practical applications since the realistic impedance usually contains noise. In this regard, we test the robustness by adding a certain level of noise into the synthetic impedance of the integrated circuit model (Fig. 1d). There are several patterns of noise embedded in the impedance. In this work, a Gaussian noise with a std. dev. (σ) is added into each real and imaginary impedance datum. Fig. 3 shows the imaginary impedances (the 1st row), the Kramers-Kronig errors for the imaginary impedance (the 2nd row) and the DRT functions by the new approach and the conventional approach (the 3rd row) at the various σ levels of $R_p/10000$, $R_p/1000$ and $R_p/100$. R_p is 0.29 Ωcm^2. For the case $\sigma = R_p/10000$, the Kramers-Kronig errors are about ±0.02%. The new approach performs fairly well. For the case $\sigma = R_p/1000$, the Kramers-Kronig errors are about ±0.3%. The new approach is still stable with respect to noise. However, for $\sigma = R_p/10000$ and $\sigma =$

R_p/1000, the DRT by the conventional approach exhibits pseudo peaks at $10^5 \sim 10^7$ Hz. For the case $\sigma = R_p/100$, the Kramers-Kronig errors are about ±4%. The processes can still be resolved correctly by the new approach, while a pseudo peak appears around 10^7 Hz. However, the conventional approach is invalid at this case. Overall, the new approach is promising for analyzing noise contaminated impedance.

The second case study is the application in a symmetric LSCF/SDC/LSCF cell. To prepare the SDC electrolyte, the SDC powders were uniaxially pressed into disk-shaped pellets at 250 Mpa, using a 13mm diameter stainless steel die, and then sintered at 1400 °C for 5 h in air to form dense SDC pellets with a diameter of about 10.0 mm and thickness of about 0.5 mm. To prepare the electrode layers, LSCF slurry (LSCF powders mixed well with α-terpineol and ethyl cellulose) was symmetrically deposited onto both sides of the substrates using the screen-printing technique. After drying under an infrared lamp, the sandwich fresh bodies were then co-fired at 1000 °C for 2 h to form symmetrical cell structures. Silver wires were attached to both sides of the symmetrical cell with silver paste (SRISR DAD-87) for current collection. The EIS of the cell was measured at 600 ºC in air with a frequency range of 0.1 Hz to 1 MHz and a bias voltage of 10 mV, using a Solartron 1260 Frequency Response Analyzer combined with a Solartron 1287 potentiostat.

Fig. 4a shows the Nyquist plot of the cell impedance. The half-tear shaped arc is representative to the coupling of surface exchange of oxygen and the transport of oxygen ions within the porous LSCF electrodes, which could be simulated by the G element [14, 17]. The DRT curves by the new approach and the conventional approach

are shown in Fig. 4b. From the DRT by the new approach, the peak located at ~ 10 Hz in the reconstructed DRT function exhibits features corresponding to the G element, such as the discontinuity/peak around 10 Hz and the monotonic decrease in DRT function beyond 10 Hz. To the best knowledge of the authors, it is the first time to identify a G element process of impedance by reconstructed DRT function without making postulation. Another peak, located at ~ 2 Hz, may be attributed to the gas diffusion process or the charge transfer of oxygen ions across LSCF/SDC interface, which are facile and usually invisible in the impedance [11]. From the DRT function by the conventional approach, The features of G element process are not obvious since there are several peaks.

Fig. 4c and d show the application of the new approach in a Ni-YSZ/YSZ/LSM-YSZ single cell. In our previous study, we have reconstructed the DRT function of the cell impedance using the conventional approach [5]. The experimental procedure is available in ref. [5]. Here we apply the new approach to resolve the electrochemical processes in the cell. Fig. 4c shows the comparison between the original and back-calculated impedances at various anode atmospheres and good agreements are observed. It is challenging to identify the number of processes by the imaginary plot of impedance shown in Fig. 4c. However, the reconstructed DRT functions by the new approach at the various anode atmospheres, shown in Fig. 4d, demonstrate clearly eight processes. By the conventional approach in our previous study [5], P1 is resolved clearly; P2 is not obviously visible; P3 and P4 merge into one peak; P5-7 merge into one peak; and the width of P8 is broader. Based on the case study shown in Figs. 1 and 3, the accuracy

and the robustness of the new approach have been verified. Thus, the more peaks resolved by the new approach are not likely the pseudo ones. However, as known, more peaks can also be generated by the conventional Tikhonov method by decreasing the regularization factor. But the pseudo peaks are usually generated. The nature of P1 is identified as the gas diffusion within the Ni/YSZ anode, validated by the 3D imaging analysis in our previous study [5]. P2-8 may relate to the transport of oxygen ions and electrons within the material bulks, the surface exchange of oxygen molecules at the material surfaces, the charge transfer of oxygen ions and electrons across the interfaces, and gas transport within the pores. As shown in Fig. 4d, P1 and P3-5 are changing with the anode atmosphere, indicating that they could be attributed to anode processes. P2 and P6-8 remain unchanged. Thus, they could be attributed to cathode processes since the atmosphere in cathode side is unchanged. Referring to the Fig. 8 in ref. [5], however, all the peaks in the DRT curves by the conventional approach change with anode side atmosphere, posing challenges in differentiating anode and cathode processes. With the merit of high precise of the new approach, the anode processes and the cathode processes for the cell can be separated by simply tailoring the anode side atmosphere. The gas diffusion resistance within the anode (P1) can be represented by the area enclosed by P1, calculated as 0.0711 Ωcm^2, 0.0612 Ωcm^2 and 0.0559 Ωcm^2 for H1N4, H2N3 and H3N2, respectively. The gas diffusion resistance decreases with the increasing of H_2 content, in agreement with our previous results [5] and the results by ref. [18]. It notes that the resistances of P3-5 decrease with the increasing of H_2 content, in agreement with our previous results [5] but different from the results by ref. [18].

The contrary results may be caused by the difference in measurement conditions or cell assembly.

Without loss of generality, the new approach can be extended to a generic formulation. Similar to DRT, there is no guarantee that the DRF is analytical. That is, the DRF may also contain discontinuities. Thus, a higher order DRF may be applicable to regularize the DRF. Thus, the generic regularization could be given by,

$$err = \left(\mathbf{\Gamma F - Z}\right)^{\mathrm{T}}\left(\mathbf{\Gamma F - Z}\right) + \left(\mathbf{D}_0\mathbf{F}\right)^{\mathrm{T}} diag\left(\boldsymbol{\lambda}_0\right)^2\left(\mathbf{D}_0\mathbf{F}\right) + \mathbf{F}^{\mathrm{T}}\mathbf{F}\sum_{i=0}^{n}\left[\left(\mathbf{D}_{i+1}\boldsymbol{\lambda}_i\right)^{\mathrm{T}} diag\left(\boldsymbol{\lambda}_{i+1}\right)^2\left(\mathbf{D}_{i+1}\boldsymbol{\lambda}_i\right)\right] \quad (3)$$

Apparently, Eq. 2 is a first-order approximation of Eq. 3 (n = 0 and $\boldsymbol{\lambda}_1 = \mathbf{1}$). The higher order approaches (n> 0 and $\boldsymbol{\lambda}_{n+1} = \mathbf{1}$) are expected to show more information of electrochemical processes.

Conclusions

We propose a new Tikhonov approach free of adjusting parameters to reconstruct the DRT function from EIS. The optimal DRT and DRF can be obtained simultaneously using a well-established algorithm. Through case studies for application in synthetic and realistic EIS, the present approach is capable of eliminating the pseudo peaks and capturing the discontinuities in the DRT function, thus demonstrating a high precision.

Acknowledgments

We gratefully acknowledge the financial support from Natural Science Foundation of China (51402066 and 51371070), the Fundamental Research Funds for the Central Universities (Grant No. HIT. NSRIF. 20167), China Postdoctoral Science Foundation funded project (2015M571410), and a grant from Science and Technology on Advanced Composites in Special Environment Laboratory of Harbin Institute of Technology.

References

[1] J.S.M. E. Barsoukov, Impedance spectroscopy theory, experiment, and applications, Second ed., John Wiley & Sons, Inc., Hoboken, New Jersey, 2005.

[2] B.T. Mark E. Orazem, Electrochemical impedance spectroscopy, John Wiley & Sons, Inc., Hoboken, New Jersey, 2008.

[3] H. Schichlein, A.C. Müller, M. Voigts, A. Krügel, E. Ivers-Tiffée, J. Appl. Electrochem. 32 (2002) 875-882.

[4] Y. Zhang, Y. Chen, M. Yan, F. Chen, J. Power Sources 283 (2015) 464-477.

[5] Y. Zhang, Y. Chen, F. Chen, J. Power Sources 277 (2015) 277-285.

[6] A. Leonide, B. Rüger, A. Weber, W.A. Meulenberg, E. Ivers-Tiffée, J. Electrochem. Soc. 157 (2010) B234-B239.

[7] B. Liu, H. Muroyama, T. Matsui, K. Tomida, T. Kabata, K. Eguchi, J. Electrochem. Soc. 157 (2010) B1858-B1864.

[8] M. Kornely, A. Neumann, N.H. Menzler, A. Leonide, A. Weber, E. Ivers-Tiffée, J. Power Sources 196 (2011) 7203-7208.

[9] T. Ramos, M. Søgaard, M.B. Mogensen, J. Electrochem. Soc. 161 (2014) F434-F444.

[10] M. Saccoccio, T.H. Wan, C. Chen, F. Ciucci, Electrochim. Acta 147 (2014) 470-482.

[11] A. Leonide, SOFC Modelling and parameter identification by means of impedance spectroscopy (PhD. dissertation), Karlsruher Institute of Technology,2010.

[12] F. Ciucci, C. Chen, Electrochim. Acta 167 (2015) 439-454.

[13] R.M. Fuoss, J.G. Kirkwood, J. Am. Chem. Soc. 63 (1941) 385-394.

[14] J.M. Esteban, M.E. Orazem, J. Electrochem. Soc. 138 (1991) 67-76.

[15] S.B. Adler, Chem. Rev. 104 (2004) 4791-4844.

[16] http://cn.mathworks.com/help/optim/ug/constrained-nonlinear-optimization-algorithms.html.

[17] S.B. Adler, J.A. Lane, B.C.H. Steele, J. Electrochem. Soc. 143 (1996) 3554-3564.

[18] A. Leonide, J. Apel, E. Ivers-Tiffée, ECS Trans. 19 (2009) 81-109.

Figure Captions

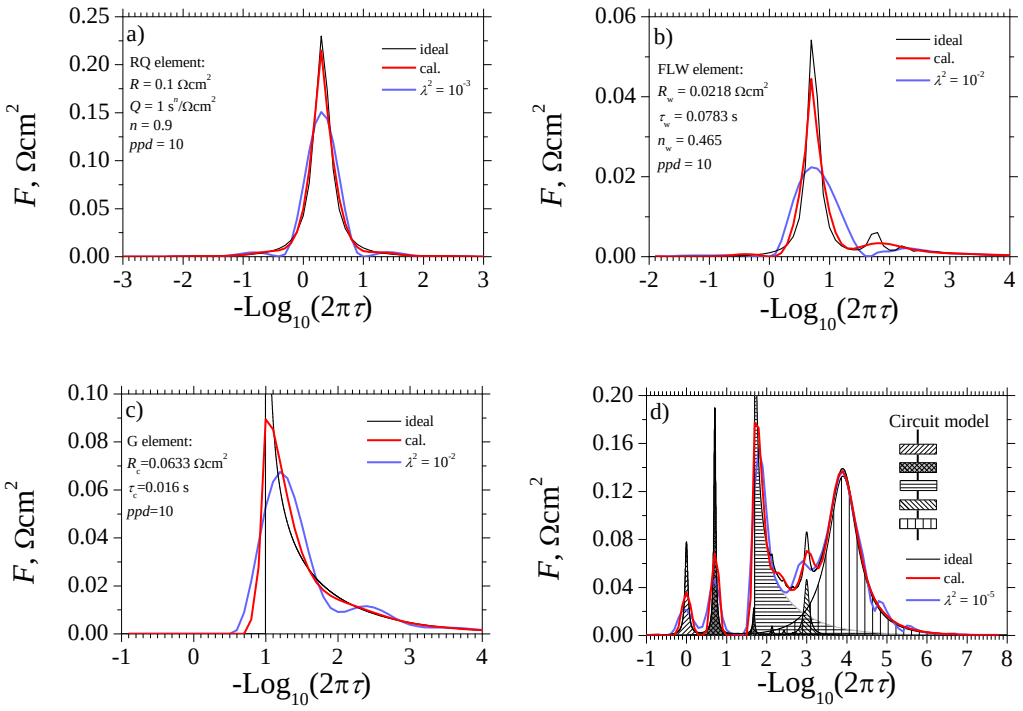

Figure 1. Comparison between the calculated DRT solutions using the new Tikhonov regularization (red curves) and the conventional Tikhonov regularization (blue curves) and the ideally analytic DRT solutions (black curves) for the RQ element (a), FLW element (b), G element (c), and the circuit model consisting of five series elements with physical quantities representative to a solid oxide fuel cell (d, P1(RQ): R = 0.01 Ωcm^2, n = 0.97, Q = 16.82 s^n/Ωcm^2; P2(FLW): R_w = 0.02 Ωcm^2, T_w = 0.0783 s, n_w = 0.49; P3(G): R_c = 0.1 Ωcm^2, τ_c = 0.0032 s; P4(RQ): R = 0.01 Ωcm^2, n = 0.95, Q = 0.0246 s^n/Ωcm^2; P5(RQ): R = 0.15 Ωcm^2, n = 0.75, Q = 0.002 s^n/Ωcm^2). The shaded patterns in (d) represent the analytic DRT solutions of the individual elements. The regularization factor λ^2 of the conventional approach is given by the averaged DRF value of the new approach in order to show a fair comparison between the two

approaches.

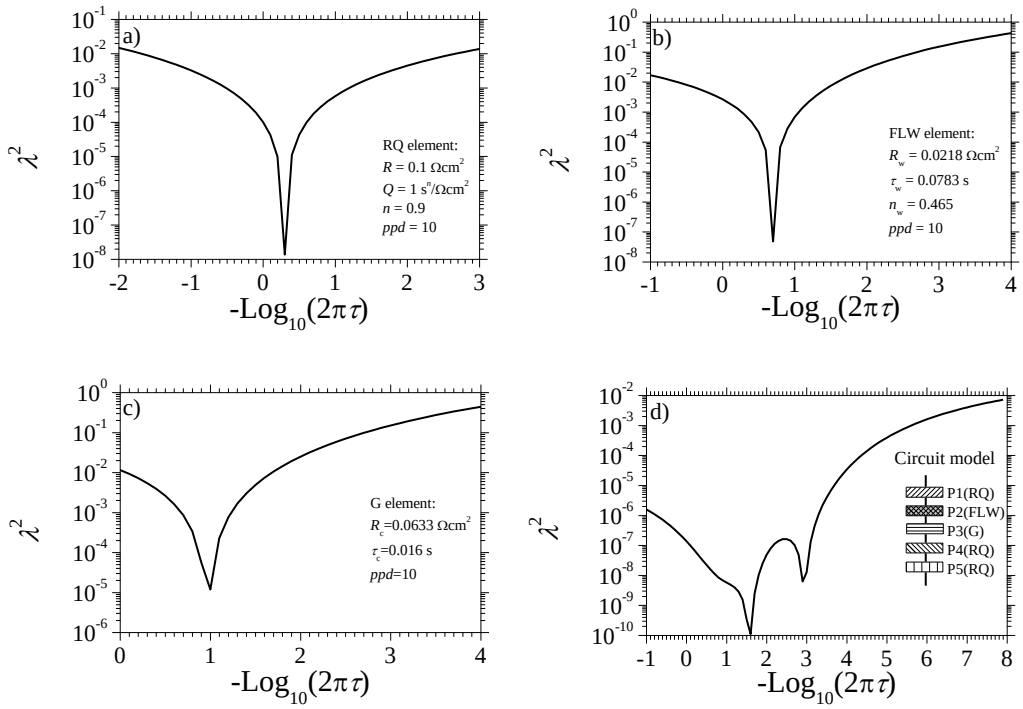

Figure 2. The calculated DRF for the RQ element (a), FLW element (b), G element (c), and the circuit model consisting of five series elements with physical quantities representative to a solid oxide fuel cell (d, P1(RQ): R = 0.01 Ωcm^2, n = 0.97, Q = 16.82 s^n/Ωcm^2; P2(FLW): R_w = 0.02 Ωcm^2, T_w = 0.0783 s, n_w = 0.49; P3(G): R_c = 0.1 Ωcm^2, τ_c = 0.0032 s; P4(RQ): R = 0.01 Ωcm^2, n = 0.95, Q = 0.0246 s^n/Ωcm^2; P5(RQ): R = 0.15 Ωcm^2, n = 0.75, Q = 0.002 s^n/Ωcm^2).

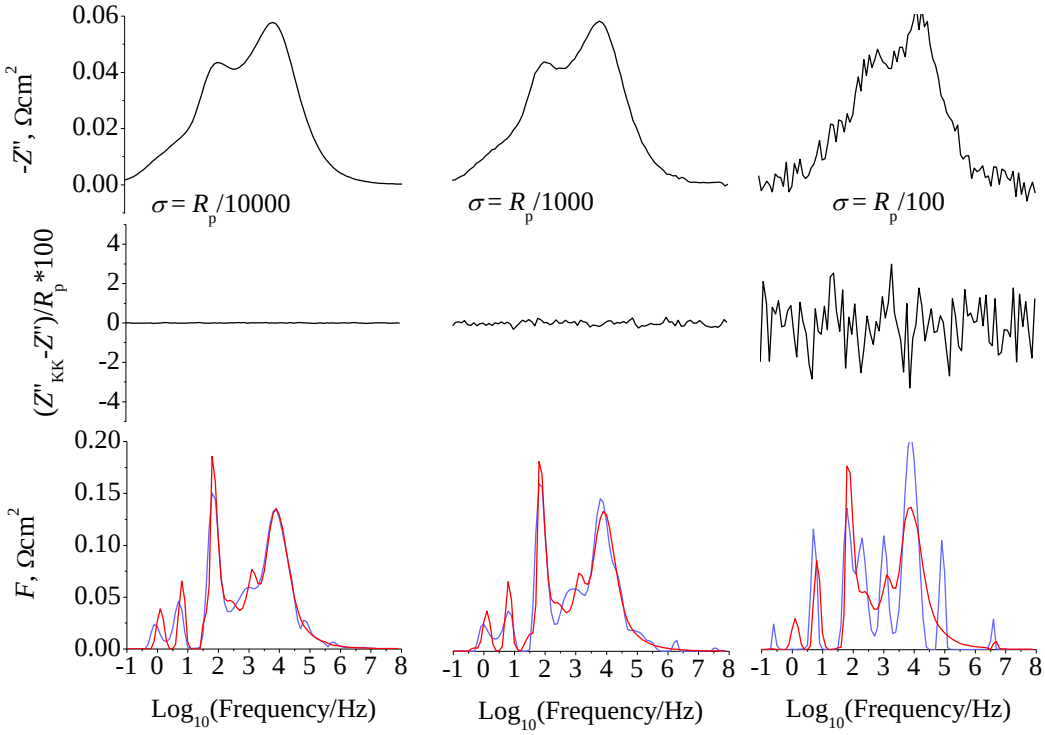

Figure 3. Imaginary part of the circuit model impedance shown in Fig. 1d embedded with different levels of std. dev. (σ) for each data point, the corresponding Kramers-Kronig test results and the calculated DRT by the present approach (the red curves) and the conventional Tikhonov regularization approach with $\lambda^2 = 10^{-5}$ (the blue curves).

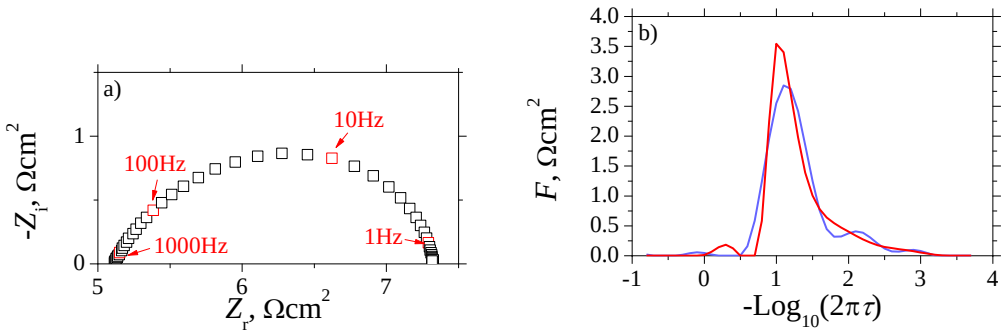

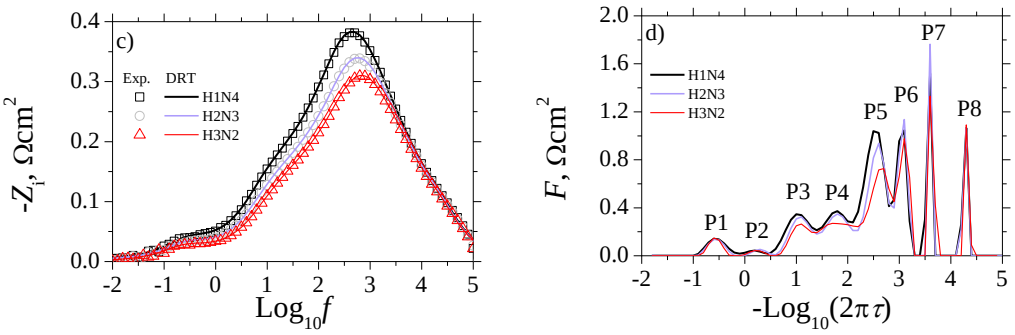

Figure 4. Nyquist plot of the impedance (a) and the calculated DRT using the new Tikhonov regularization (red curve) and the conventional Tikhonov regularization with $\lambda^2 = 10^{-3}$ (blue curve) (b) for the symmetric LSCF/SDC/LSCF solid oxide cell under open circuit at 600 ºC in air. Imaginary part of impedances by experiments (scatters) and the one back-calculated by DRT solutions (lines) (c) and the calculated DRT solutions (d) of the Ni-YSZ/YSZ/LSM-YSZ solid oxide cell under open circuit at 750 ºC in the various anodic gas mixtures of H_2-N_2-H_2O. H*a*N*b* represents that the molar ratio of H_2/N_2 is *a*/*b* (balanced with 3% H_2O). The cathode atmosphere is air.